DEMO-HEP-97/04
hep-ph/9703372
March 1997

Leptoquark production at LEP2

Costas G. Papadopoulos

Institute of Nuclear Physics, NCSR $\Delta\eta\mu\acute{o}\kappa\rho\iota\tau o\varsigma$, 15310 Athens, Greece

ABSTRACT

We study the production of scalar and vector leptoquarks at high-energy e^+e^- colliders. All leptoquark contributions into semileptonic four-fermion final states have been calculated and incorporated in the Monte Carlo event generator ERATO. Taking into account the irreducible Standard Model backgrounds we invetsigate the potential of LEP2 for studying leptoquarks.

Revised version May 1997

E-mail: Costas.Papadopoulos@cern.ch.

The reported excess of high Q^2 events at HERA by the H1 [1] and ZEUS [2] collaborations stimulated a substantial research interest on the possible existence of new particles of leptoquark type. Such particles emerge in several contexts, including the Pati-Salam model [3] and the grand-unified supersymmetric theories [4]. Leptoquark-type interactions, described by higher-dimensional contact terms, are naturally incorporated within the idea of compositeness of quarks and leptons [5].

Although the current HERA data are not yet conclusive[1] [1, 2] and no unambiguous interpretation exists [7, 8, 9, 10], it is rather important to ask the question whether LEP2 will be able to sed some light on this issue. In this paper we present the calculation of all tree-order leptoquark contributions to four fermion final states at high-energy e^+e^- colliders. This automatically includes pair leptoquark production as well as single leptoquark production channels. As an application we present results concerning the contribution of leptoquark states in four-fermion production processes at LEP2.

We start the presentation with the most general effective Lagrangian [11], which is $SU(3)\times SU(2)\times U(1)$ invariant, baryon- and lepton-number conserving as well as family diagonal, in order to avoid the most severe constraints from low-energy considerations [12]. It can be written as

$$\begin{aligned}\mathcal{L}_{F=-2} &= \left(g_{0L}\,\bar{q}_L^c i\tau_2\ell_L + g_{0R}\,\bar{u}_R^c e_R\right) S_0 + \tilde{g}_{0R}\,\bar{d}_R^c e_R \tilde{S}_0 + g_{1L}\,\bar{q}_L^c i\tau_2\vec{\boldsymbol{\tau}}\ell_L \vec{S}_1 \\ &+ \left(g_{\frac{1}{2}L}\,\bar{d}_L^c\gamma^\mu\ell_L + g_{\frac{1}{2}R}\,\bar{q}_L^c\gamma^\mu e_R\right) V_{\frac{1}{2}\mu} + \tilde{g}_{\frac{1}{2}L}\,\bar{u}_R^c\gamma^\mu\ell_L\tilde{V}_{\frac{1}{2}\mu} + \text{cc} \qquad (1)\end{aligned}$$

$$\begin{aligned}\mathcal{L}_{F=0} &= \left(h_{\frac{1}{2}L}\,\bar{u}_R\ell_L + h_{\frac{1}{2}R}\,\bar{q}_L i\tau_2 e_R\right) S_{\frac{1}{2}} + \tilde{h}_{\frac{1}{2}L}\,\bar{d}_R\ell_L\tilde{S}_{\frac{1}{2}} + \tilde{h}_{0R}\,\bar{u}_R\gamma^\mu e_R\tilde{V}_{0\mu} \\ &+ \left(h_{0L}\,\bar{q}_L\gamma^\mu\ell_L + h_{0R}\,\bar{d}_R\gamma^\mu e_R\right) V_{0\mu} + h_{1L}\bar{q}_L\vec{\boldsymbol{\tau}}\gamma^\mu\ell_L\vec{V}_{1\mu} + \text{cc} \qquad (2)\end{aligned}$$

where $F = 3B + L$ denotes the fermion number. The gauge-interaction terms are given by

$$\mathcal{L} = (D_\mu\boldsymbol{\Phi})^\dagger D^\mu\boldsymbol{\Phi} - M^2\boldsymbol{\Phi}^\dagger\boldsymbol{\Phi} \qquad (3)$$

for scalars and

$$\mathcal{L} = -\frac{1}{2}G^\dagger_{\mu\nu}G^{\mu\nu} + M^2\boldsymbol{\Phi}^\dagger_\mu\boldsymbol{\Phi}^\mu \qquad (4)$$

for vectors, with

$$G_{\mu\nu} = D_\mu\boldsymbol{\Phi}_\nu - D_\nu\boldsymbol{\Phi}_\mu \qquad (5)$$

and the $SU(2)_L\times U(1)_Y$ covariant derivative given by

$$D_\mu = \left[\partial_\mu - ieQ^\gamma A_\mu - ieQ^Z Z_\mu - ieQ^W(W^+_\mu I^+ + W^-_\mu I^-)\right] \qquad (6)$$

[1] See for instance reference [6] for a further discussion.

where $I^{\pm}$ are the $SU(2)$ generators in the representation of the corresponding leptoquark state. The electroweak charges are given by

$$Q^Z = \frac{I_3 - Q^\gamma \sin^2\theta_w}{\cos\theta_w \ \sin\theta_w} \tag{7}$$

and

$$Q^W = \frac{1}{\sqrt{2}\sin\theta_w} \ . \tag{8}$$

In order to account for a more general structure in the vector leptoquark case one can also add the so called 'anomalous couplings' terms as for instance the 'magnetic' dipole one given by

$$\mathcal{L}_{extra} = -i \sum_{V=\gamma,Z} g_V \kappa_V \boldsymbol{\Phi}^\dagger_\mu V^{\mu\nu} \boldsymbol{\Phi}_\nu \tag{9}$$

parametrized in terms of κ_γ and κ_Z.

Leptoquark contributions to e^+e^- processes can be classified into real and virtual ones. To the lowest order, virtual contributions proceed via the reaction $e^+e^- \to q\bar{q}$ [7, 8, 10], whereas for real ones we have the single leptoquark production mode [13, 14, 15] and for light enough masses, or high enough energies, the pair leptoquark production [16].

Leptoquark production at high-energy e^+e^- collisions results to a four-fermion final state. We have calculated all tree-order contributions, including all interference terms with the Standard Model, to the following 'semileptonic' reactions

$$e^-e^+ \to \ell^-\ell^+ q\bar{q} \tag{10}$$

and

$$e^-e^+ \to \ell^-\bar{\nu}_\ell q\bar{q}' \ , \tag{11}$$

where $\ell = e, \mu, \tau$. A full description of the MC generator `ERATO` as well as its present extension can be found in references [17, 18]. Leptoquark contributions to $\nu_\ell\bar{\nu}_\ell q\bar{q}$ and $q\bar{q}q'\bar{q}'$ final states have not been considered here, since, as we will see, they are relatively suppressed.

For the first reaction, Eq.(10), with $\ell = e$ ($\ell = \mu, \tau$), the Standard Model Feynman graphs are of the `NC48` (`NC24`) type[2], whereas the leptoquark contribution can be classified in two categories: the `LQ22` (`LQ11`), which is diagrammatically identical to the Standard Model `CC22` (`CC11`) with the W boson replaced by a leptoquark, and a new category, called `EQ20`, which contributes only when $\ell = e$. The generic graphs belonging to the

[2]For the nomenclature about the four-fermion production diagrams see reference [18].

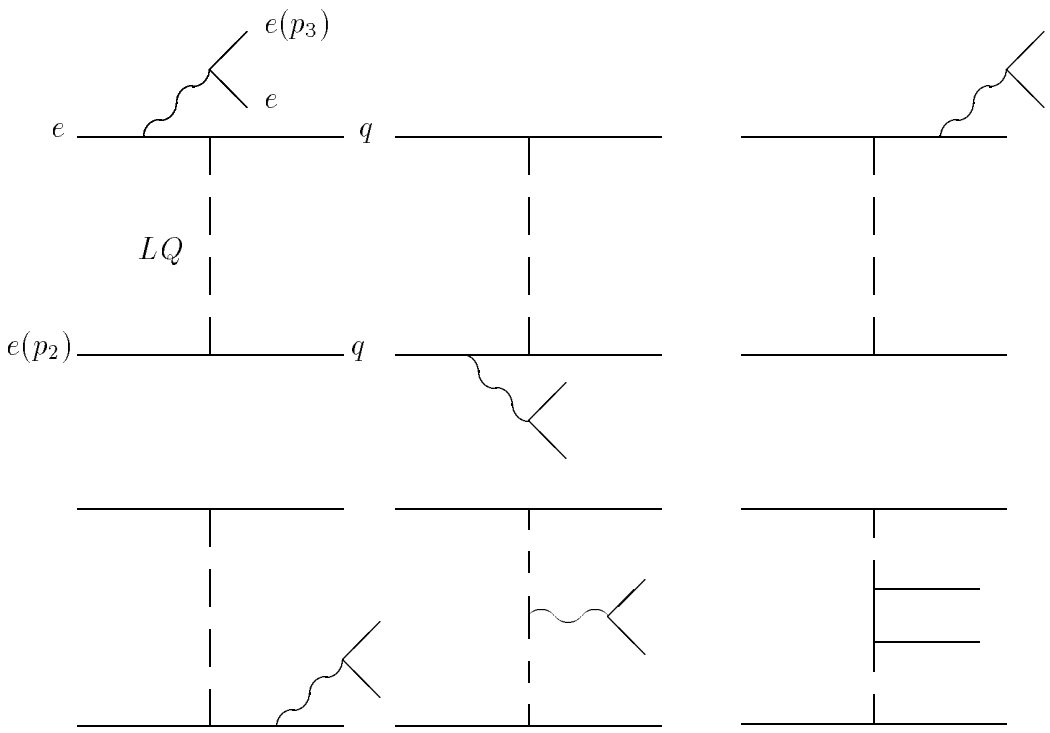

Figure 1: `EQ20`, `EQ10` and `EQ5` classes. The curly lines can be γ, Z or W, with the appropriate changes in the fermion species. The other half of the graphs are obtained, as usually, by the interchange $e(p_2) \leftrightarrow e(p_3)$.

latter class are shown in Fig.1. Moreover there are nine scalar and nine vector leptoquark states contributing to these processes, namely

$$S_0^L, S_0^R, \tilde{S}_0^R, S_{1+}^L, S_{10}^L, S_{\frac{1}{2}+}^L, S_{\frac{1}{2}+}^R, S_{\frac{1}{2}-}^R \text{ and } \tilde{S}_{\frac{1}{2}+}^R$$

and

$$V_{\frac{1}{2}+}^L, V_{\frac{1}{2}+}^R, V_{\frac{1}{2}-}^R, \tilde{V}_{\frac{1}{2}+}^R V_0^L, V_0^R, \tilde{V}_0^R, V_{1+}^L \text{ and } V_{10}^L \,,$$

with the obvious notation X_{bc}^a, where $a = L, R$ is the helicity of the lepton, $b = I$ is the isospin of the leptoquark and $c = I_3$ stands for its third component.

For the reaction Eq.(11), Standard Model contributions belong to the well known `CC20`(`CC10`) category, whereas those of leptoquarks fall into three different classes. The first one is the `LQ20`(`LQ10`), in close analogy to the previous case. The other two, the `EQ10` and `EQ6`, Fig.1, receive contributions only from the first generation leptoquarks. In the `LQ20`(`LQ10`) class only $S_0^L, \vec{S}_1^L$ and $U_0^L, \vec{U}_1^L$ states contribute, whereas in the classes `EQ10` and `EQ6` we have contributions from S_1^L, V_1^L and $S_{\frac{1}{2}}^R$, $V_{\frac{1}{2}}^R$ respectively.

In addition to the calculation of all tree-order Feynman graphs, we have also employed all phase-space mappings [19, 17], which are necessary to cover all the kinematical regions where leptoquarks have the most substantial contributions. Initial state radiation (ISR) has also been included in the structure function approach [20]. Our calculation provides therefore the necessary framework to investigate real leptoquark production at high-energy e^+e^- colliders, including both pair- and single-production modes, for all leptoquark types, as given by Eq.(1)-Eq.(2), and for all generations. Nevertheless we find it convenient, in the light of recent data from HERA, to focus our present analysis on the first generation leptoquarks. It should be mentioned, however, that all necessary contributions for the study of the 2nd and 3rd generation leptoquarks at LEP2 have been fully accounted for in the present calculation and incorporated in `ERATO`.

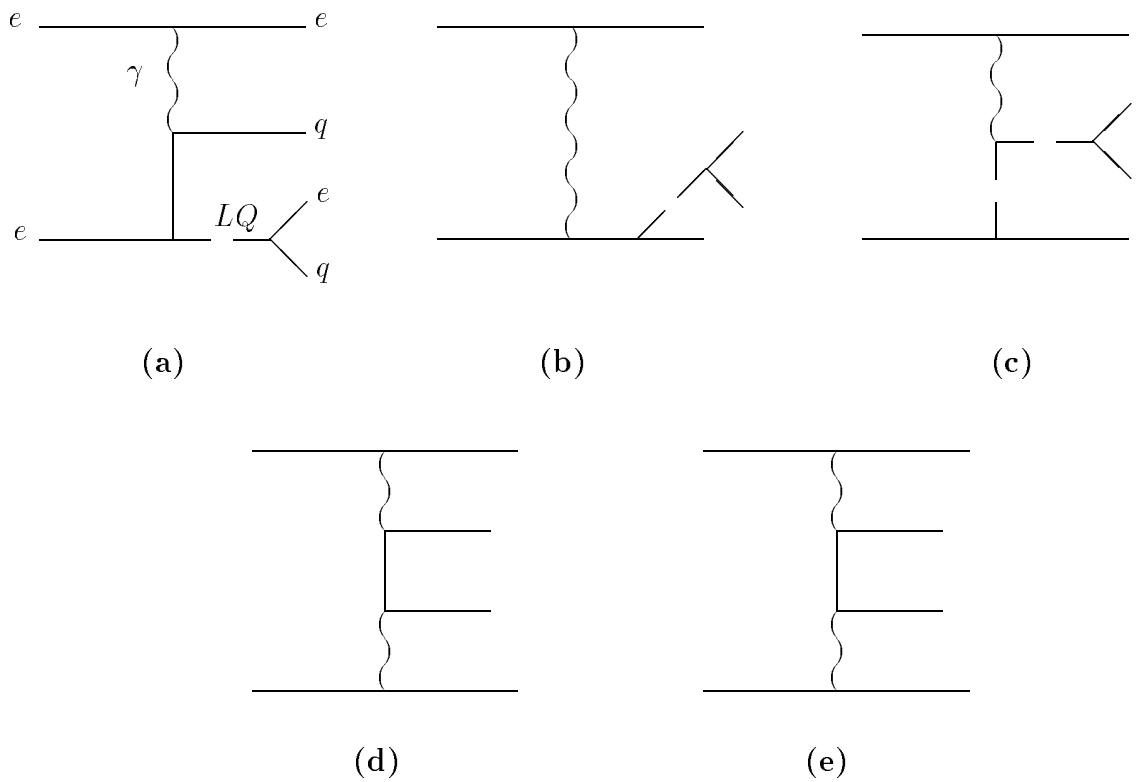

Figure 2: The subset of Feynman graphs giving the dominant contribution to single leptoquark production: (a,b,c) signal, (e,d) background.

Although leptoquark contributions appear in a large number of graphs only a small

part of them give a sizable contribution to the production cross-section, depending of course on the leptoquark parameters such as the mass and the Yukawa coupling. The first important consideration is coming from the total width of the leptoquark, which is given by

$$\Gamma_J = f_J \, \frac{M}{8\pi} \, \sum_{i=1}^{N_{ch}} \lambda_i^2 \tag{12}$$

where $J = 0, 1$ is the spin of the particle, $f_0 = \frac{1}{2}$ and $f_1 = \frac{1}{3}$ and $N_{ch} = 1$ or 2 depending on how many channels are available. As is evident for a leptoquark mass of the $\mathcal{O}(200$ GeV) the typical width is of the order of a few hundreds of MeV. This is mainly due to the fact that leptoquarks couple to ordinary fermions in a very restricted way, which is not generally true for other types of leptoquark couplings, like those appearing in R-parity violating MSSM [7]. As a consequence of the narrowness of these states the interference terms among resonant ans non-resonant contributions are rather suppressed.

The second remark is that, for leptoquark masses $M \geq \sqrt{s}/2$, the single leptoquark production mode becomes dominant as far as the first generation leptoquarks are concerned. This proceeds mainly via the t-channel graphs, shown in Fig.2, and their contribution comes mainly from the collinear electrons (positrons). This can be described either by the Weizsäcker-Williams [21] approximation or by integrating over the momentum of the final state electron using the leading logarithmic approximation as described in reference [19]. We have implemented *both* approaches, and checked that the results agree within less that 10%, which is rather typical for the leading logarithmic (LL) approximation we are essentially employing in both cases. As far as the Weizsäcker-Williams spectrum is concerned, we have used the following form:

$$f_\gamma(x) = \frac{\alpha}{2\pi} \left[\frac{1 + (1-x)^2}{x} \ln \left(\frac{s}{m_e^2} \frac{(1-x)^2}{(2-x)^2} \right) + x \ln \frac{2-x}{x} + \frac{2(x-1)}{x} \right] \quad . \tag{13}$$

It should be mentioned that this type of contributions, which are substantially enhanced due to the t-channel photon exchange, are only relevant for the first generation leptoquarks and for the semileptonic reactions, Eq.(10)-Eq.(11), under consideration. On the other hand, first generation leptoquark contributions to $\nu_\ell \bar{\nu}_\ell q \bar{q}$ and $q \bar{q} q' \bar{q}'$ final states are relatively suppressed, due to the absence of the t-channel photon exchange enhancement.

Finally, as the first graph of Fig.2 has a mass singularity in the quark propagator, special care has to be paid in the integration in this specific case. As before the LL-approximation scheme has been employed. It is worth to mention that comparing with the exact result for the total cross-section [14], taking fully into account the quark masses, and properly integrating over the photon spectrum, both results agree to less than a few percent.

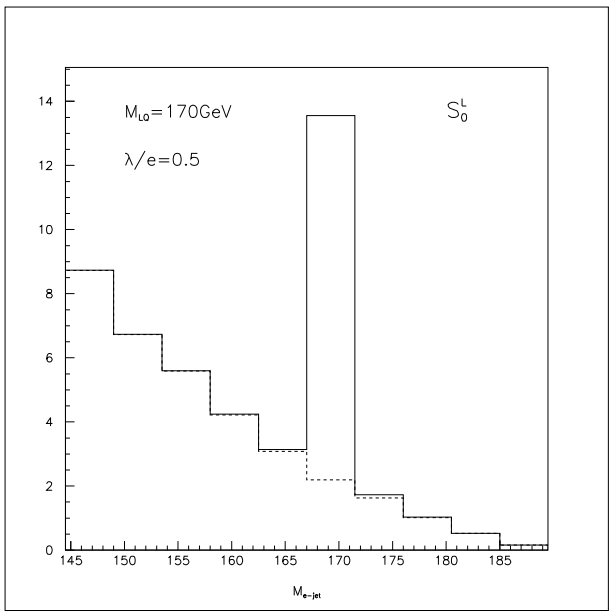

Figure 3: The m_{e-jet} invariant mass distribution in number of events ber bin.

After completing the description of our calculation, we now come to the physics picture emerging from it. In the case of NC-type final states, Eq.(10), the signal has the typical structure of a lepton and a jet balancing each other's transverse momentum with some hadronic activity in the forward (backward) region. In the irreducible Standard Model background, on the other hand, the angular distribution of the positron (electron) is peaking in the backward (forward) direction. In order to suppress as much as possible the background, without lowering signal's contribution, we have employed the following set of cuts:

$$m_{e-jet} \geq 140 \text{ GeV} \ , \ \ 5^o \leq \max(\theta_{j1}, \theta_{j2}) \leq 175^o \ , \ \ 20^o \leq \theta_e \leq 160^o \ , \ \ E_e \geq 5 \text{ GeV} \ . \quad (14)$$

Among them the most important ones are the cut on the angle of the observed positron (electron) and the cut on the electron-jet invariant mass, m_{e-jet}. In Fig.3 we show the invariant mass, m_{e-jet}, distribution for leptoquark mass $M = 170$ GeV and $\lambda/e = 0.5$, with an integrated luminosity $L = 500$ pb^{-1}. Assuming now an invariant mass resolution[3] of 5 GeV, we show in Fig.4 the 95% CL bounds in the leptoquark parameter space $\lambda - M$.

[3]As is evident from Fig.3 our results do not depend drastically on this value.

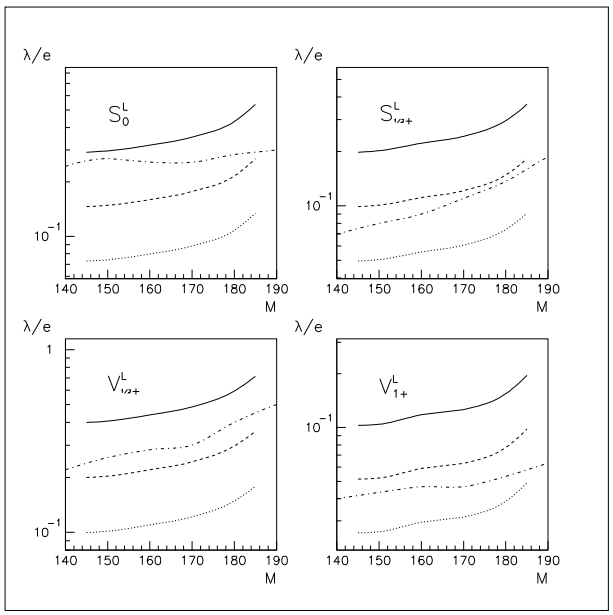

Figure 4: The 95% CL limits from single leptoquark production in the NC channel at $\sqrt{s} = 192$ GeV and for integrated luminosities of 500 pb^{-1} (solid), 1 fb^{-1} (dashed) and 2 fb^{-1} (dotted). Also shown (dot-dashed) are the current limits from HERA[22].

In the case of CC-type final states, Eq.(11), the signal, which is much more spectacular, consists only of one very energetic jet and a large amount of missing transverse energy. The only cuts employed in this case are

$$\max(p_{T1}, p_{T2}) \geq 60 \text{ GeV} \quad , \quad \min(\theta_{j1}, \theta_{j2}) \leq 5^o \text{ or } \geq 175^o \ , \tag{15}$$

where p_T is the transverse energy of the jet. The second cut is employed in order to reduce the main irreducible background contribution, coming from single W production, in which case two energetic jets, with an invariant mass $\mathcal{O}(M_W)$, would be present in the final state at relatively large angles with respect to the beam. Moreover, as the only kinematical information available in this channel is the jet momentum, one cannot fully reconstruct the mass of the leptoquark state, due to the missing neutrino energy[4]. In Fig.5 we show the p_T spectrum of the signal as well as that of the irreducible Standard Model background. Taking into account the total number of expected/observed events, Fig.5 shows the 95% CL bounds in the plane $\lambda - M$. It should be mentioned that CC-channels are less useful, compared to the NC ones, for leptoquark searches, for two reasons:

[4]However the leptoquark mass can still be determined by the endpoint of the p_T spectrum.

the first is that only a few states contribute to these channel and the second is that their contribution is suppressed by the reduced branching ratio.

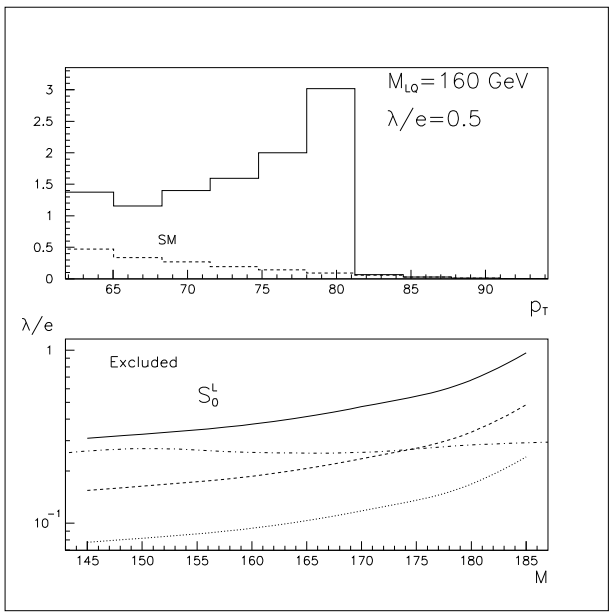

Figure 5: Upper part: the p_T distribution in number of events per bin. Lower part: the 95% (solid) CL limits in the CC channel, as in Fig.4.

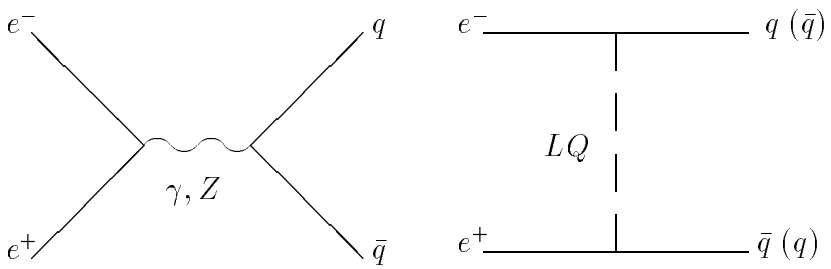

Figure 6: The contribution to two-jet production.

Virtual leptoquark contributions to the high-energy e^+e^- collisions can be studied in the two-jet production channel. The Feynman graphs contributing are shown in Fig.6. Leptoquarks appear in the t(u)-channel exchange graphs and their contribution looks more or less like a contact term. We have calculated the helicity amplitudes using the

Feynman rules implied by the Lagrangian Eq.(1)-Eq.(2) including initial state radiation (ISR) via the structure function approach [20]. In order to simulate as much as possible the actual experimental conditions and to reduce the background from the radiative return of the Z, the following cuts have been applied,

$$\sqrt{s'} \geq 160\text{GeV} \quad , \quad 5^o \leq \theta_{jet} \leq 175^o \quad . \tag{16}$$

In order to evaluate the sensitivity of this process to leptoquark parameters we have used an unbinned extended maximum likelihood (EML) fit which produces essentially the best achievable result, assuming that the 'data' are fully accounted for by the Standard Model contributions. The 95% CL limits are shown in Fig.7 for several scalar and vector leptoquark types. The conclusion is that the two-jet production at LEP2 will be able to explore the high leptoquark mass region well beyond the HERA limits [22]. Note that although no hadronization neither experimental resolution effects have been taken into account in the present analysis, we do not expect that the physical picture will be qualitatively affected.

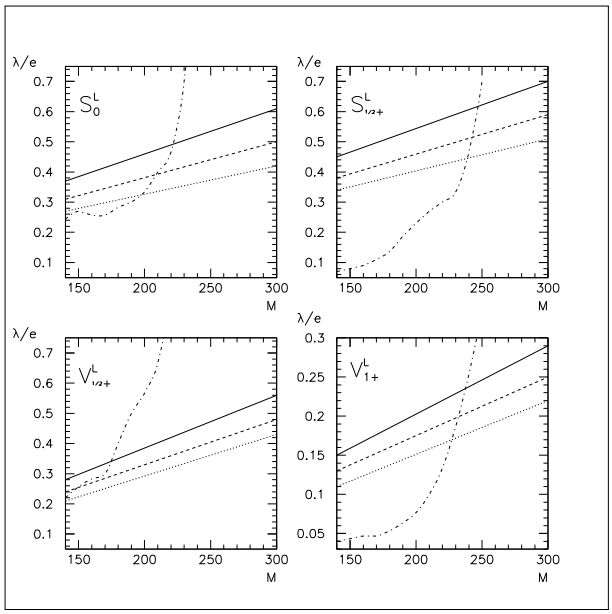

Figure 7: The 95% CL limits from two-jet production, as in Fig.4.

In summary, we have presented a calculation of leptoquark contributions to two- and four-fermion final states at e^+e^- collisions, which has been incorporated in the MC event generator `ERATO`. Taking into account the Standard Model irreducible backgrounds we

have studied leptoquark production, in both its NC or CC channel, and we investigated the parameter space in which LEP2, operating at $\sqrt{s} = 192$ GeV and with integrated luminosities from 500 pb^{-1} up to 2 fb^{-1} would be sensitive. Our results show that a higher luminosity, few times the planned one, is needed in order to substantially improve on the current HERA limits. Furthermore, since the analysis is more or less translationally invariant in the energy scale, an increase of the overall energy, i.e. form $\sqrt{s} = 192$ GeV to $\sqrt{s} = 205$ GeV, would result to a proportional increase in the leptoquark mass limits. It is also important to note that the studies of real leptoquark production and of the virtual leptoquark contribution to the two-jet cross section are complementary, with the former being more efficient for $M \leq \sqrt{s}$ and the latter being able to extend LEP2 sensitivity beyond the overall collision energy.

References

[1] H1 Collaboration, C.Adloff *et al.*, DESY 97-024, hep-ex/9702012.

[2] ZEUS Collaboration, J.Breitweg *et al.*, DESY 97-025, hep-ex/9702015.

[3] J.C. Pati and A. Salam, Phys. Rev. **D8** (1973) 1240; *ibid* **D10** (1974) 275.

[4] H. Georgi and S.L. Glashow, Phys. Rev. Lett. **32** (1974) 438; P.Langacker, Phys. Rep. **72** (1981) 185 ; E.Witten, Nucl. Phys. **B258** (1985) 75; J.L. Hewett and T.G. Rizzo, Phys. Rep. **193** (1989) 193

[5] L. Abbot and E. Farhi, Phys. Lett. **B101** (1981) 69; W. Buchmüller, Acta Phys. Austr. Suppl. XXVII (1985)517; H. Harari and N. Seiberg, Phys. Lett. **B98** (1981) 269; S. Adler, IASSNS-HEP-97/12, hep-ph/9702378.

[6] M. Drees, APCTP 97-03, hep-ph/9703332.

[7] D. Choudhury, S. Raychaudhuri, CERN-TH/97-26, hep-ph/9702392; G. Altarelli *et al.*, CERN-TH/97-40, hep-ph/9703276; H. Dreiner and P. Morawitz, hep-ph/9703279.

[8] J. Kalinowski, R. Rückl, H. Spiesberger and P.M. Zerwas, BI-TP 97/07, DESY 97-038, WUE-ITP-97-02, hep-ph/9703288.

[9] J. Blümlein, DESY 97-032, hep-ph/9703287; K.S. Babu, C. Kolda, J. March-Russel, and F. Wilczek, IASSNS-HEP-97-04, hep-ph/9703299; V. Barger, K. Cheung, K. Hagiwara and D. Zeppenfeld, MADPH-97-991, hep-ph/9703311.

[10] J.L. Hewett and T.G. Rizzo, SLAC-PUB-7430, hep-ph/9703337.

[11] W. Buchmüller, R. Rückl and D. Wyler, Phys. Lett. **B191** (1987) 442.

[12] M. Leurer, Phys. Rev. **D49** (1994) 333; *ibid* **D50** (1994) 536.

[13] M.A. Doncheski and S. Godfrey, OCIP/C 96-1, hep-ph/9608368; OCIP/C 97-02, hep-ph/9703285.

[14] G. Bélanger, D. London and H. Nadeau, Phys. Rev. **D49** (1994) 3140.

[15] T.M. Aliev, E. Iltan and N.K. Pak, Phys. Rev. **D54** (1996) 4263.

[16] J. Blümlein and R. Rückl, Phys. Lett. **B304** (1993) 337 and references therein; J. Blümlein, E. Boos and A .Kryukov, Phys. Lett. **B392** (1997) 150.

[17] Costas G. Papadopoulos, Comp.Phys.Comm. **101** (1997) 183. ftp://alice.nrcps.ariadne-t.gr/pub/papadopo/erato.

[18] D. Bardin *et al.*, 'Event generators for WW physics' in *Physics at LEP2*, ed. G. Altarelli *et al.*, Vol.2, p. 3, CERN 96-01, February 1996.

[19] F.A.Berends, R.Pittau and R.Kleiss, Nucl.Phys.**B424**(1994) 308.

[20] W. Beenakker *et al.*, 'WW cross sections and distributions' in *Physics at LEP2*, ed. G. Altarelli *et al.*, Vol.1, p. 79, CERN 96-01, February 1996 & hep-ph/9602351.

[21] C.F. von Weizsäcker, Z. Phys. **88**(1934), 612; E.J. Williams, Phys. Rev. **45** (1934) 729; M. Chen and P. Zerwas, Phys. Rev. **D12** (1975) 187.

[22] H1 Collaboration, S. Aid *et al.*, Phys. Lett. **B369** (1996) 173.